

Nonlinear topological phase transitions in the dimerized sine-Gordon model

Motohiko Ezawa *Department of Applied Physics, University of Tokyo, Hongo 7-3-1, 113-8656, Japan*

(Received 29 October 2021; revised 13 February 2022; accepted 5 April 2022; published 15 April 2022)

The nonlinear system is a frontier of topological physics. As a prototype, we propose the dimerized sine-Gordon model by combining the sine-Gordon model and the Su-Schrieffer-Heeger model. It has rich varieties of phases depending on the nonlinearity and the dimerization. This system is realized by a simple system of coupled pendulums, which is an ideal playground to explore associated intriguing phenomena. They are observable by the quench dynamics starting from the left-end pendulum. The topological and trivial phases are well defined for the weak nonlinear regime, where a pendulum motion is well approximated by a harmonic oscillator. The emergence of the topological edge state is detected by the standing waves whose amplitude exponentially decays with stationary even-numbered pendulums. In addition, we find nonlinearity-induced phases, i.e., the trap phase with a strictly localized standing wave and the dimer phase with a few coupled standing waves trapped to the left end. We also study a nonlinear dimerized Duffing model, which is obtained by the third-order Taylor expansion of the dimerized sine-Gordon model.

DOI: [10.1103/PhysRevB.105.165418](https://doi.org/10.1103/PhysRevB.105.165418)

I. INTRODUCTION

Topological physics is extensively studied in condensed-matter physics [1,2]. The topological phase is signaled by the emergence of topological edge states. Now, the target of topological physics has expanded to artificial topological systems such as acoustic [3–12], mechanical [13–29], photonic [30–37], and electric circuit [38–48] systems. The merit of artificial topological systems is that system parameters can be finely controlled. In addition, it is possible to make a small sample with clean edges.

Topological physics has been mainly studied in linear systems. Recently, the frontier of the study of topological phases has reached nonlinear systems. Nonlinear effects are naturally introduced in artificial topological systems. In this context, topological physics in nonlinear systems is studied in mechanical [49–52], photonic [53–61], electric circuit [62,63], and resonator [64] systems. It is an interesting problem how the topological phases are modified in the presence of the nonlinear term. Furthermore, it is fascinating if there is a phase transition induced by the nonlinear term.

In this paper, we study topological physics in nonlinear systems analytically and numerically. As a simplest system, we propose the dimerized sine-Gordon model, which is defined by dimerizing the sine-Gordon model with the alternative coupling strengths $\kappa_A = \kappa(1 + \lambda)$ and $\kappa_B = \kappa(1 - \lambda)$ with $|\lambda| \leq 1$. It is reduced to the sine-Gordon model as $\lambda \rightarrow 0$. It is intriguing that the model contains the Su-Schrieffer-Heeger (SSH) model in its parts, and hence we expect the emergence of topological and trivial phases. We explore a phase diagram by studying quench dynamics, where we impose an initial condition $\phi_n(t) = \xi\pi\delta_{n,1}$ and $\dot{\phi}_n(t) = 0$ on the sine-Gordon fields ϕ_n with the index $n = 1$ representing the left-end site. We may use ξ as a nonlinearity parameter.

Indeed, it is possible to define the topological number in the weak nonlinear regime $|\xi| \ll 1$ by the first-order perturbation theory with respect to ξ . The system is topological with the emergence of the topological edge states for $\lambda < 0$, while it is trivial for $\lambda > 0$. Beyond the weak nonlinear regime we determine phases by studying the quench dynamics numerically. It is found that the phase boundary is quite insensitive to the initial condition for $|\xi| \lesssim 1/2$. The nonlinearity effect becomes dominant for $|\xi| \gtrsim 1/2$, and eventually the system turns into the nonlinearity-induced trap phase.

The dimerized sine-Gordon model is realized physically by a coupled pendulum system with alternating torsion as illustrated in Fig. 1. We give an oscillation only to the left-end pendulum initially and investigate a quench dynamics of how the oscillation propagates to other pendulums. We set the initial swing angle $\xi\pi$ at the left-end pendulum, where $|\xi| \leq 1$. The pendulum motion is well approximated by a harmonic oscillator for $|\xi| \ll 1$. This system possesses topological and trivial phases. The topological phase is signaled by the characteristic oscillation with parity, where the amplitude exponentially decays along the chain direction but with the even-numbered pendulums kept almost stationary as in Fig. 1(b).

We have found four phases, which we explain with the use of a coupled pendulum system. First, we have the topological phase, where a few left-end, odd-numbered pendulums show simple standing waves, representing the topological edge state. Second, we have the trivial phase, where the oscillation propagates into the bulk. Third, the system turns into the trap phase in the strong nonlinear regime, where the oscillation occurs as a perfectly localized standing wave at the left-end pendulum. This is because the interaction between adjacent pendulum is negligible with respect to the nonlinear localization effect. Forth, we find the dimer phase, where coupled

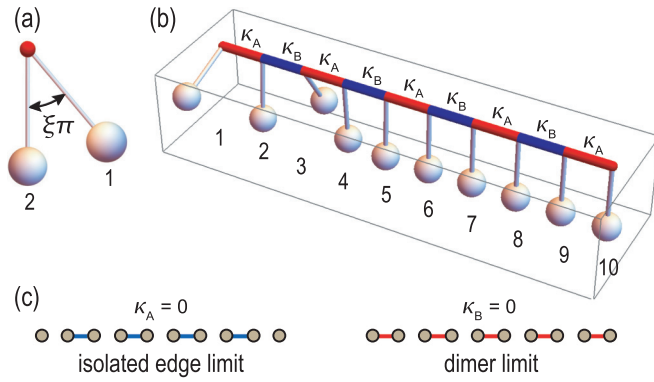


FIG. 1. Illustration of coupled pendulums. Adjacent pendulums are connected by a wire which has a restoring force depending on the angle difference. The torsion is alternating as $\kappa_A = \kappa(1 + \lambda)$ and $\kappa_B = \kappa(1 - \lambda)$. The system is described by the dimerized sine-Gordon equation. (a) Horizontal view of the initial condition (11). (b) Bird's eye's view of a chain of pendulums in the topological phase, where $g/\kappa = 1$, $\lambda = -0.5$ and $\xi = 0.5$. The pendulum at $n = 2$ is stationary. (c) Illustration of the isolated edge limit and the dimer limit.

standing waves are trapped to a few pendulums at the left end. Its dynamical origin is the cooperation of the dimerization and the nonlinear term.

We have also made a similar analysis of a nonlinear dimerized Duffing model, which is obtained by the third-order Taylor expansion of the dimerized sine-Gordon model. The phase diagram is found to be quite similar to the one in the dimerized sine-Gordon model.

II. DISCRETE SINE-GORDON MODEL

A typical nonlinear system is the sine-Gordon model described by

$$m \frac{d^2 \phi}{dt^2} = \kappa \frac{\partial^2 \phi}{\partial x^2} - g \sin \phi. \quad (1)$$

By discretizing it on a one-dimensional chain, we obtain a discrete sine-Gordon model [65,66], where the equation of motion is given by

$$m \frac{d^2 \phi_n}{dt^2} = \kappa [\phi_{n+1} + \phi_{n-1} - 2\phi_n] - g \sin \phi_n. \quad (2)$$

It is rewritten in the form of

$$m \frac{d^2 \phi_n}{dt^2} + g \sin \phi_n - \sum_{nm} M_{nm} \phi_m = 0, \quad (3)$$

where M_{nm} is the hopping matrix with the coupling κ ,

$$M_{nm} = \kappa (\delta_{n,m+1} + \delta_{n,m-1} - 2\delta_{n,m}). \quad (4)$$

Equation (3) is derived from the Lagrangian

$$L = \sum_n \left[m \left(\frac{d\phi_n}{dt} \right)^2 + g \cos \phi_n \right] + \sum_{nm} M_{nm} \phi_n \phi_m. \quad (5)$$

The corresponding Hamiltonian is

$$H = \sum_n \left[m \left(\frac{d\phi_n}{dt} \right)^2 - g \cos \phi_n \right] - \sum_{nm} M_{nm} \phi_n \phi_m, \quad (6)$$

which is a conserved energy.

III. DIMERIZED SINE-GORDON MODEL

We generalize the system by making the matrix M_{nm} equipped with a nontrivial topological structure. As a simplest example, we propose the dimerized sine-Gordon model, where the matrix is given by the SSH model. The equation of motion is given by Eq. (3) together with the hopping matrix

$$M_{nm} = -(\kappa_A + \kappa_B) \delta_{n,m} + \kappa_A (\delta_{2n,2m-1} + \delta_{2m,2n-1}) + \kappa_B (\delta_{2n,2m+1} + \delta_{2m,2n+1}). \quad (7)$$

The Lagrangian of the system is given by Eqs. (5) with (7), which we refer to as the dimerized sine-Gordon model.

The explicit equations are given by

$$m \frac{d^2 \phi_{2n-1}}{dt^2} = \kappa_A (\phi_{2n} - \phi_{2n-1}) + \kappa_B (\phi_{2n-2} - \phi_{2n-1}) - g \sin \phi_{2n-1}, \quad (8)$$

$$m \frac{d^2 \phi_{2n}}{dt^2} = \kappa_B (\phi_{2n+1} - \phi_{2n}) + \kappa_A (\phi_{2n-1} - \phi_{2n}) - g \sin \phi_{2n}. \quad (9)$$

It is convenient to introduce the coupling strength κ and the dimerization parameter λ by

$$\kappa_A = \kappa(1 + \lambda), \quad \kappa_B = \kappa(1 - \lambda), \quad (10)$$

with $|\lambda| \leq 1$.

A. Mechanical system realization

We discuss how to realize the dimerized sine-Gordon model experimentally. It is realized by a mechanical system shown in Fig. 1, where coupled pendulums are connected by wires. Each pendulum rotates perpendicular to the wire direction. Here m is an inertia moment of the pendulum and g is the gravitational acceleration constant. The alternating hopping coefficients κ_A and κ_B are introduced by the torsion of the wire connecting two pendulums. Then, M_{nm} given by Eq. (7) is a matrix representing the couplings between the n -th and the m -th pendulums. A wire has a restoring force against the force induced by the angle difference between the two adjacent pendulums.

B. Quench dynamics

Quench dynamics starting from a localized state is a good signal to detect whether the system is topological or trivial [67]. We analyze a quench dynamics in the present system, where we solve the dimerized sine-Gordon equation under the initial condition,

$$\phi_n(t) = \xi \pi \delta_{n,1} \quad \text{and} \quad \dot{\phi}_n(t) = 0 \quad \text{at} \quad t = 0, \quad (11)$$

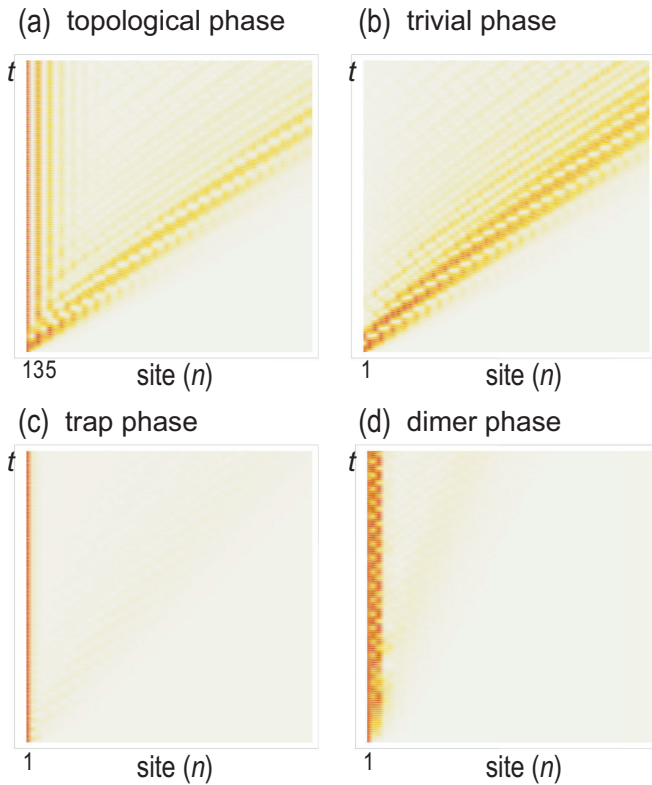


FIG. 2. Time evolution of the amplitude ϕ_n of the n -th pendulum. (a) The topological phase with $\lambda = -0.25$ and $\xi = 0.1$, where there are simple standing waves for odd-numbered pendulums. (b) The trivial phase with $\lambda = 0.25$ and $\xi = 0.1$, where the oscillation propagates along the chain. (c) The trap phase with $\lambda = 0.5$ and $\xi = 0.75$, where the standing wave is present only at the left-end pendulum. (d) The dimer phase with $\lambda = 0.75$ and $\xi = 0.5$, where coupled standing waves are trapped to a few pendulums at the left end. We have set $g/\kappa = 10$.

where $|\xi| \leq 1$. Namely, we set the initial angle of the left-end pendulum to be $\xi\pi$ and all the others to be zero in a chain of pendulums as illustrated in Fig. 1(a). Then, allowing it to move with the zero initial velocity under the gravitational force, we study how the motion propagates along the chain as in Fig. 1(b).

We treat the coupling strength κ , the dimerization parameter λ , and the initial condition ξ as the system parameters. We have studied the quench dynamics for a variety of these parameters. We have found there are four types of solutions numerically, whose typical structures are given in Fig. 2.

In Fig. 2(a), there are standing waves mainly at the left-end pendulum and weakly at a few adjacent odd-number pendulums, and furthermore there are propagating waves into the bulk with a constant velocity. In Fig. 2(b), there are only propagating waves into the bulk with a constant velocity. In Fig. 2(c), the standing wave is trapped strictly at the left-end pendulum. In Fig. 2(d), the coupled standing waves are trapped to a few pendulums at the left end.

In general, it is impossible to solve the dimerized sine-Gordon equation analytically. Nevertheless, it is possible to obtain analytical results locally to explain these behaviors.

C. Topological and trivial phases

First, we make a change of variable, $\phi_n = \xi\phi'_n$, and rewrite Eq. (3) as

$$m \frac{d^2 \phi'_n}{dt^2} = \sum_m M_{nm} \phi'_m - \frac{g}{\xi} \sin \xi \phi'_n, \quad (12)$$

with the initial condition

$$\phi'_1(0) = \pi. \quad (13)$$

By taking the limit $\xi \rightarrow 0$, Eq. (12) is reduced to a linear equation,

$$m \frac{d^2 \phi'_n}{dt^2} = \sum_m \bar{M}_{nm} \phi'_m, \quad (14)$$

where we have redefined the hopping matrix as

$$\bar{M}_{nm} \equiv M_{nm} - g\delta_{n,m}. \quad (15)$$

Actually, it is a very good approximation to set $\sin \xi\phi'_n \simeq \xi\phi'_n$ in the vicinity of $\xi = 0$. We call such a parameter region the weak nonlinear regime, where the nonlinear equation (3) is well approximated by Eq. (14). Physically, this corresponds to the case where the pendulum is approximated by a harmonic oscillator.

Equation (14) is the SSH model with a modified matrix \bar{M}_{nm} . As described in the Appendix, the present model (14) has the same phases as the SSH model. The system is topological for $\lambda < 0$ and trivial for $\lambda > 0$ in the weak nonlinear regime.

The topological phase is characterized by the emergence of zero-mode edge states for a finite chain. In the linearized equation (14), the zero-mode edge state is solved as

$$\phi_{2n+1} = \left(-\frac{\kappa_A}{\kappa_B} \right)^n \phi_1, \quad \phi_{2n} = 0. \quad (16)$$

It has the major component in the left-end pendulum but also has components in a few adjacent odd-numbered pendulums. Now, the initial motion is given only to the left-end pendulum, which is only a part of the zero-mode edge state. This mismatch allows some parts to propagate into the bulk with the velocity $\sim \sqrt{\kappa/m}$, while those within the zero-mode edge state stay as they are, exhibiting standing waves. Thus this analytic solution well describes the structure made of standing waves and propagating waves, as shown in Fig. 2(a), where $\lambda = -0.25$ and $\xi = 0.1$.

On the other hand, there is no zero-mode edge state in the trivial phase. Hence the left-end pendulum motion propagates entirely into the bulk, which well explains the structure made of propagating waves with the velocity $\sim \sqrt{\kappa/m}$ in Fig. 2(b), where $\lambda = 0.25$ and $\xi = 0.1$.

D. Trap phase

We next study the limit where the nonlinear term is dominant over the hopping term in Eq. (3), where we may approximate it as

$$m \frac{d^2 \phi_n}{dt^2} = -g \sin \phi_n. \quad (17)$$

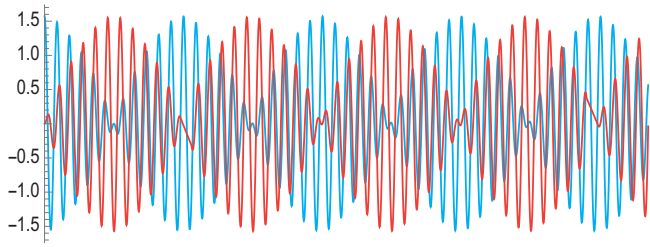


FIG. 3. Time evolution of the angle ϕ_1 and ϕ_2 in the dimer phase ($\lambda = 1$) under the initial condition $\phi_1 = \pi/2$ and $\phi_2 = 0$. We have set $g/\kappa = 10$.

We call such a parameter region the strong nonlinear regime, where the nonlinear equation (3) is well approximated by Eq. (17).

The prominent feature of the strong nonlinear regime is that all equations are perfectly decoupled. Each is a simple pendulum equation, whose exact solution is given by

$$\phi_n = 2 \sin^{-1}[\alpha_n \text{sn}(\omega t, \alpha_n)], \quad (18)$$

where sn is the Jacobi elliptic function, $\omega \equiv \sqrt{g/m}$ and α_n is determined as $\alpha_n = \sin[\phi_n(0)/2]$ in terms of the initial condition $\phi_n(0)$. Under the initial condition (11), the left-end pendulum makes a motion described by Eq. (18) with $n = 1$ while all other pendulums remain stationary. The pendulum motion is perfectly trapped to the left end of the chain, as explains the structure made of a single standing wave in Fig. 2(c), where $\lambda = 0.5$ and $\xi = 0.75$.

E. Dimer phase

We consider the limit $\lambda = 1$, where the system is perfectly dimerized. In this case, the equations of motion are given by

$$m \frac{d^2 \phi_1}{dt^2} = \kappa_A (\phi_2 - \phi_1) - g \sin \phi_1, \quad (19)$$

$$m \frac{d^2 \phi_2}{dt^2} = \kappa_A (\phi_1 - \phi_2) - g \sin \phi_2. \quad (20)$$

Solving this set of equations numerically under the initial condition $\phi_1 = \xi\pi$ and $\phi_2 = 0$, we show the results in Fig. 3, where the set of oscillatory waves with long and short periods appears for ϕ_1 and ϕ_2 .

The above analysis is correct only in the limit $\lambda = 1$. In general, a coupling is present between the dimer and the adjacent pendulum. Numerical calculation shows coupled standing waves trapped to a few pendulums at the left end as in Fig. 2(d), where $\lambda = 0.75$ and $\xi = 0.5$. Taking this coupling into account, the above set of beat oscillatory waves accounts for the pendulum motion near the limit $\lambda = 1$.

F. Phase diagram

We have performed a numerical calculation of the quench dynamics for the left-end pendulum in a wide range of system parameters, where we have used the parameter ξ to control the nonlinearity. We show the value of the amplitude ϕ_1 of the left-end pendulum after enough time as a function of the dimerization λ and the initial phase ξ in Fig. 4. We have set $g/\kappa = 10$ so that the system belongs to the strong nonlinear regime around $\xi = 1$.

Figure 4(b) presents a rough picture of the phase diagram. The phase boundary is determined by the characteristic behaviors of the phase indicator, which is the normalized swing angle $\phi_1/\xi\pi$. We calculate it as a function of ξ for a fixed value λ or as a function of λ for a fixed value ξ , whose results are shown for some typical values of λ and ξ in Fig. 5. In general, the phase transition point is given by the position of a gap in the phase indicator as in Fig. 5. On the other hand, the typical behavior separating the topological and trivial phases is given in Fig. 5(c), where the phase indicator is finite in the topological phase and decreases smoothly to zero in the trivial phase [52,60,63]. Note that $\phi_1 = 0$ in the trivial phase of the semi-infinite system. We have constructed the phase diagram in Fig. 4(c) by determining the phase boundaries according to these criteria.

We find four distinct phases: (1) The topological phase, (2) the trivial phase, (3) the trap phase, and (4) the dimer phase. The distinction between the topological and the trivial phases is clear analytically in the weak nonlinear regime ($\xi \simeq 0$). We have found numerically that this topological phase boundary does not change in spite of the increase of the nonlinear term up to $\xi \lesssim 0.5$. On the other hand, there is a nonlinearity-induced trap phase in the strong nonlinear regime ($\xi \simeq 1$). We have found numerically that the trap phase appears even for $\xi \gtrsim 0.6$. There is another phase in the vicinity of $\lambda = 1$, which is the dimer phase.

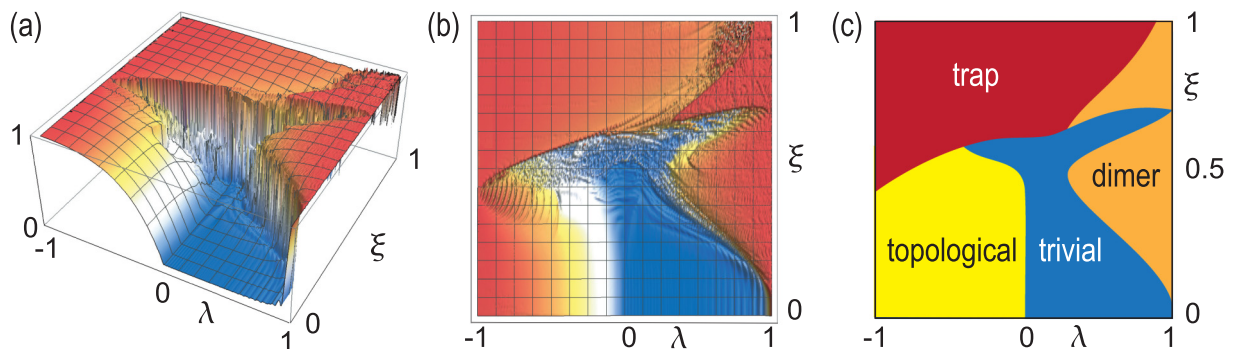


FIG. 4. Normalized swing angle $\phi_1/\xi\pi$ of the left-end pendulum after enough time as a function of the dimerization λ and the initial condition ξ . (a) Bird's eye's view. (b) Top view. (c) Phase diagram of the dimerized sine-Gordon model. We have set $g/\kappa = 10$.

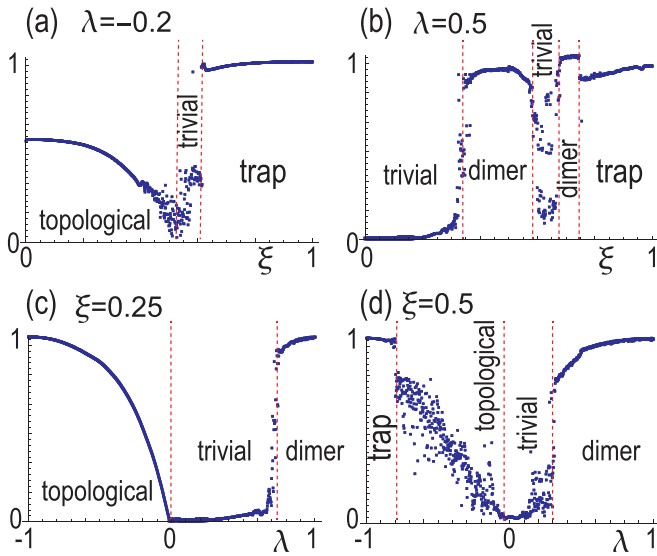


FIG. 5. Normalized swing angle $\phi_1/\xi\pi$ as a function of ξ at (a) $\lambda = -0.2$ and (b) $\lambda = 0.5$ and that as a function of λ at (c) $\xi = 0.25$ and (d) $\xi = 0.5$. We have set $g/\kappa = 10$. A gap indicates a phase transition point in general. The trivial phase is characterized by $\phi_1 = 0$ in the semi-infinite system. Various phases are indicated in figures.

IV. NONLINEARITY PARAMETERS

We have constructed the phase diagram in the (λ, ξ) plane by fixing $g/\kappa = 10$ in Fig. 4. This is because the system does not reach the strong nonlinear regime when g/κ is small. It is necessary to investigate the condition imposed on ξ and g/κ for the strong nonlinear regime to be realized. Examining the quench dynamics, we construct the phase diagram in the $(\xi, g/\kappa)$ plane by fixing $\lambda = 0.1$. The result is shown in Fig. 6(a), which shows that both ξ and g/κ should be appropriately large.

It is actually possible to construct the phase diagram in the $(\lambda, g/\kappa)$ plane by fixing ξ appropriately. We show such a phase diagram in Fig. 6(b), where we have chosen $\xi = 1$. The overall structure is identical to the phase diagram in the (λ, ξ) plane in Fig. 4.

Hence, both ξ and g/κ characterize the nonlinear term. However, it is easier to change the initial condition ξ than the

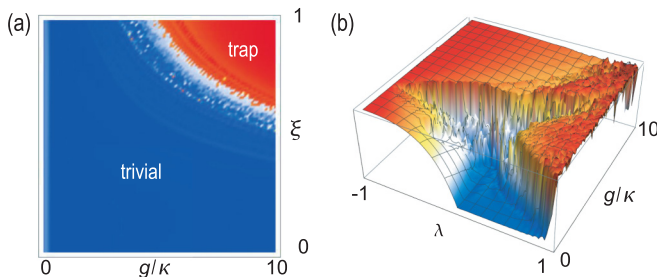


FIG. 6. (a) Normalized swing angle $\phi_1/\xi\pi$ in the $(g/\kappa, \xi)$ plane at fixed $\lambda = 0.01$. (b) Bird's eye's view of the normalized swing angle $\phi_1/\xi\pi$ in the $(\lambda, g/\kappa)$ plane at fixed $\xi = 1$.

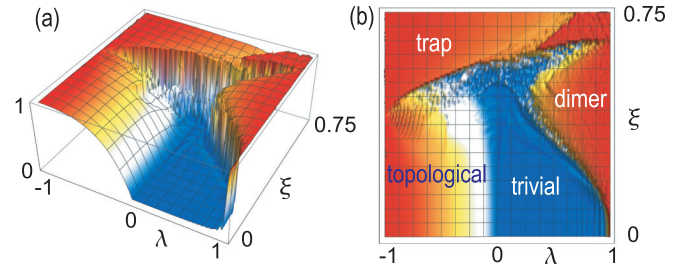


FIG. 7. Normalized swing angle $\phi_1/\xi\pi$ of the left-end pendulum after enough time as a function of the dimerization λ and the initial condition ξ in the Duffing model. (a) Bird's eye's view. (b) Top view, representing the phase diagram of the dimerized Duffing model. We have set $g/\kappa = 10$.

parameter g/κ , where κ represents the hopping constant and g the gravitational constant in the case of coupled pendulums.

V. DIMERIZED DUFFING OSCILLATOR

In this work, as a simplest nonlinear system, we studied the dimerized sine-Gordon model. One might consider the simplest one would be given by the dimerized Duffing model. A special case is given by

$$m \frac{d^2 \phi_n}{dt^2} + g \left(\phi_n - \frac{\phi_n^3}{6} \right) - \sum_{nm} M_{nm} \phi_m = 0, \quad (21)$$

which is obtained by making the Taylor expansion of the sine term up to the third order.

Equation (21) is derived from the Lagrangian

$$L = \sum_n \left[m \left(\frac{d\phi_n}{dt} \right)^2 + g \left(1 - \frac{\phi_n^2}{2} + \frac{\phi_n^4}{24} \right) \right] + \sum_{nm} M_{nm} \phi_n \phi_m. \quad (22)$$

The corresponding Hamiltonian is

$$H = \sum_n \left[m \left(\frac{d\phi_n}{dt} \right)^2 - g \left(1 - \frac{\phi_n^2}{2} + \frac{\phi_n^4}{24} \right) \right] - \sum_{nm} M_{nm} \phi_n \phi_m, \quad (23)$$

which is a conserved energy.

The key observation is that the potential energy becomes a negative infinity as ϕ_n becomes a positive infinity due to the ϕ_n^4 term. The system is shown to be stable provided $\phi_n < \sqrt{6}$, which is identical to $\xi < \sqrt{6}/\pi$ with the initial condition (11).

We show the phase diagram in Fig. 7 by choosing $\xi < \sqrt{6}/\pi$. In this case, the overall phase diagram is almost identical to that of the dimerized sine-Gordon model for $\xi < \sqrt{6}/\pi$. This is physically reasonable because the oscillation is restricted to be small.

VI. DISCUSSION

To explore a frontier of the topological physics in nonlinear systems, we have proposed the dimerized sine-Gordon model and constructed a phase diagram as a function of the nonlinearity and the dimerization. The phase diagram is very similar to that of the nonlinear Schrödinger systems [60] although the models are very different. Indeed, the former is the second-order differential equation with real variables, while

the latter is the first-order differential equation with complex variables.

The similarity reveals a universal feature of nonlinear topological systems. The similarity between these models is that there are two competing terms. One is the hopping term governing the topological physics in the weak nonlinear regime, and the other is the nonlinear term governing nontopological physics in the strong nonlinear regime. In the weak nonlinear regime, the system is well described by the hopping term and the topological phase boundary remains as it is. On the other hand, in the strong nonlinear limit, the system turns into a nonlinearity-induced trap phase irrespective of the dimerization parameter λ , because the hopping term does not play a significant role. In addition, there is a dimer phase, where the quench dynamics is trapped to a few pendulums at the left end.

Our results show that the quench dynamics starting from the edge is a good signal to determine a phase diagram. It is an interesting problem to study various nonlinear systems in the context of topology.

ACKNOWLEDGMENTS

M.E. is very much grateful to N. Nagaosa for helpful discussions on the subject. This work is supported by the Grants-in-Aid for Scientific Research from MEXT KAKENHI (Grants No. JP17K05490 and No. JP18H03676). This work is also supported by CREST, JST (JPMJCR16F1 and JPMJCR20T2).

APPENDIX: TOPOLOGICAL NUMBER

We discuss the topological number in the system (14), where the hopping matrix (15) is represented in the momentum space as

$$\bar{M}(k) = -(\kappa_A + \kappa_B + g)I_2 + M_0(k), \quad (\text{A1})$$

with

$$q(k) = \kappa_A + \kappa_B e^{-ik}, \quad (\text{A2})$$

and

$$M_0(k) = \begin{pmatrix} 0 & q(k) \\ q^*(k) & 0 \end{pmatrix}. \quad (\text{A3})$$

We note that the system (14) is the SSH model with the use of Eq. (A3) rather than Eq. (A1).

In the SSH model, the topological number is the Berry phase defined by

$$\Gamma = \frac{1}{2\pi} \int_0^{2\pi} A(k) dk, \quad (\text{A4})$$

where $A(k) = -i\langle \psi(k) | \partial_k | \psi(k) \rangle$ is the Berry connection with $\psi(k)$ the eigenfunction of $M_0(k)$. Because the wave function $\psi(k)$ does not depend on the diagonal term, the topological charge is given by Eq. (A4) also in the present system with $\bar{M}(k)$.

Consequently, the dimerized sine-Gordon model is topological ($\Gamma = 1$) for $\kappa_B > \kappa_A$ and trivial ($\Gamma = 0$) for $\kappa_B < \kappa_A$ in the weak nonlinear regime.

-
- [1] M. Z. Hasan and C. L. Kane, *Rev. Mod. Phys.* **82**, 3045 (2010).
 - [2] X.-L. Qi and S.-C. Zhang, *Rev. Mod. Phys.* **83**, 1057 (2011).
 - [3] E. Prodan and C. Prodan, *Phys. Rev. Lett.* **103**, 248101 (2009).
 - [4] Z. Yang, F. Gao, X. Shi, X. Lin, Z. Gao, Y. Chong, and B. Zhang, *Phys. Rev. Lett.* **114**, 114301 (2015).
 - [5] P. Wang, L. Lu, and K. Bertoldi, *Phys. Rev. Lett.* **115**, 104302 (2015).
 - [6] M. Xiao, G. Ma, Z. Yang, P. Sheng, Z. Q. Zhang, and C. T. Chan, *Nat. Phys.* **11**, 240 (2015).
 - [7] C. He, X. Ni, H. Ge, X.-C. Sun, Y.-B. Chen, M.-H. Lu, X.-P. Liu, L. Feng, and Y.-F. Chen, *Nat. Phys.* **12**, 1124 (2016).
 - [8] H. Abbaszadeh, A. Souslov, J. Paulose, H. Schomerus, and V. Vitelli, *Phys. Rev. Lett.* **119**, 195502 (2017).
 - [9] H. Xue, Y. Yang, F. Gao, Y. Chong, and B. Zhang, *Nat. Mater.* **18**, 108 (2019).
 - [10] X. Ni, M. Weiner, A. Alu, and A. B. Khanikaev, *Nat. Mater.* **18**, 113 (2019).
 - [11] M. Weiner, X. Ni, M. Li, A. Alu, A. B. Khanikaev, *Sci. Adv.* **6**, eaay4166 (2020).
 - [12] H. Xue, Y. Yang, G. Liu, F. Gao, Y. Chong, and B. Zhang, *Phys. Rev. Lett.* **122**, 244301 (2019).
 - [13] C. L. Kane and T. C. Lubensky, *Nat. Phys.* **10**, 39 (2014).
 - [14] Bryan Gin-ge Chen, N. Upadhyaya, and V. Vitelli, *Proc. Natl. Acad. Sci. USA* **111**, 13004 (2014).
 - [15] L. M. Nash, D. Kleckner, A. Read, V. Vitelli, A. M. Turner, and W. T. M. Irvine, *Proc. Natl. Acad. Sci. USA* **112**, 14495 (2015).
 - [16] J. Paulose, A. S. Meeussen, and V. Vitelli, *Proc. Natl. Acad. Sci. USA* **112**, 7639 (2015).
 - [17] R. Süsstrunk and S. D. Huber, *Science* **349**, 47 (2015).
 - [18] R. Süsstrunk and S. D. Huber, *Proc. Natl. Acad. Sci. USA* **113**, E4767 (2016).
 - [19] S. D. Huber, *Nat. Phys.* **12**, 621 (2016).
 - [20] A. S. Meeussen, J. Paulose, and V. Vitelli, *Phys. Rev. X* **6**, 041029 (2016).
 - [21] T. Kariyado and Y. Hatsugai, *Sci. Rep.* **5**, 18107 (2016).
 - [22] T. Kariyado and Y. Hatsugai, *J. Phys. Soc. Jpn.* **85**, 043001 (2016).
 - [23] H. C. Po, Y. Bahri, and A. Vishwanath, *Phys. Rev. B* **93**, 205158 (2016).
 - [24] D. Z. Rocklin, Bryan G. G. Chen, M. Falk, V. Vitelli, and T. C. Lubensky, *Phys. Rev. Lett.* **116**, 135503 (2016).
 - [25] Y. Takahashi, T. Kariyado, and Y. Hatsugai, *New J. Phys.* **19**, 035003 (2017).
 - [26] K. H. Matlack, M. Serra-Garcia, A. Palermo, S. D. Huber, and C. Daraio, *Nat. Mater.* **17**, 323 (2018).
 - [27] Y. Takahashi, T. Kariyado, and Y. Hatsugai, *Phys. Rev. B* **99**, 024102 (2019).
 - [28] A. Ghatak, M. Brandenbourger, J. van Wezel, and C. Coulais, *Proc. Natl. Acad. Sci. USA* **117**, 29561 (2020).
 - [29] H. Wakao, T. Yoshida, H. Araki, T. Mizoguchi, and Y. Hatsugai, *Phys. Rev. B* **101**, 094107 (2020).
 - [30] A. B. Khanikaev, S. H. Mousavi, W.-K. Tse, M. Kargarian, A. H. MacDonald, and G. Shvets, *Nat. Mater.* **12**, 233 (2013).
 - [31] M. Hafezi, E. Demler, M. Lukin, and J. Taylor, *Nat. Phys.* **7**, 907 (2011).

- [32] M. Hafezi, S. Mittal, J. Fan, A. Migdall, and J. Taylor, *Nat. Photonics* **7**, 1001 (2013).
- [33] L. H. Wu and X. Hu, *Phys. Rev. Lett.* **114**, 223901 (2015).
- [34] L. Lu, J. D. Joannopoulos, and M. Soljacic, *Nat. Photonics* **8**, 821 (2014).
- [35] T. Ozawa, H. M. Price, A. Amo, N. Goldman, M. Hafezi, L. Lu, M. C. Rechtsman, D. Schuster, J. Simon, O. Zilberberg, and I. Carusotto, *Rev. Mod. Phys.* **91**, 015006 (2019).
- [36] A. E. Hassan, F. K. Kunst, A. Moritz, G. Andler, E. J. Bergholtz, and M. Bourennane, *Nat. Photonics* **13**, 697 (2019).
- [37] M. Li, D. Zhirihin, D. Filonov, X. Ni, A. Slobozhanyuk, A. Alu, and A. B. Khanikaev, *Nat. Photonics* **14**, 89 (2020).
- [38] S. Imhof, C. Berger, F. Bayer, J. Brehm, L. Molenkamp, T. Kiessling, F. Schindler, C. H. Lee, M. Greiter, T. Neupert, and R. Thomale, *Nat. Phys.* **14**, 925 (2018).
- [39] C. H. Lee, S. Imhof, C. Berger, F. Bayer, J. Brehm, L. W. Molenkamp, T. Kiessling, and R. Thomale, *Commun. Phys.* **1**, 39 (2018).
- [40] T. Helbig, T. Hofmann, C. H. Lee, R. Thomale, S. Imhof, L. W. Molenkamp, and T. Kiessling, *Phys. Rev. B* **99**, 161114(R) (2019).
- [41] Y. Lu, N. Jia, L. Su, C. Owens, G. Juzeliunas, D. I. Schuster, and J. Simon, *Phys. Rev. B* **99**, 020302(R) (2019).
- [42] Y. Li, Y. Sun, W. Zhu, Z. Guo, J. Jiang, T. Kariyado, H. Chen, and X. Hu, *Nat. Commun.* **9**, 4598 (2018).
- [43] M. Ezawa, *Phys. Rev. B* **98**, 201402(R) (2018).
- [44] E. Zhao, *Ann. Phys.* **399**, 289 (2018).
- [45] M. Ezawa, *Phys. Rev. B* **99**, 201411(R) (2019).
- [46] M. Ezawa, *Phys. Rev. B* **99**, 121411(R) (2019).
- [47] M. Serra-Garcia, R. Susstrunk, and S. D. Huber, *Phys. Rev. B* **99**, 020304(R) (2019).
- [48] T. Hofmann, T. Helbig, C. H. Lee, M. Greiter, and R. Thomale, *Phys. Rev. Lett.* **122**, 247702 (2019).
- [49] R. K. Pal, J. Vila, M. Leamy, and M. Ruzzene, *Phys. Rev. E* **97**, 032209 (2018).
- [50] D. D. J. M. Snee, Y.-P. Ma, *Extreme Mech. Lett.* **30100487** (2019).
- [51] P. W. Lo, C. D. Santangelo, B. G.-g. Chen, C. M. Jian, K. Roychowdhury, M. J. Lawler, *Phys. Rev. Lett.* **127**, 076802 (2021).
- [52] M. Ezawa, *J. Phys. Soc. Jpn.* **90**, 114605 (2021).
- [53] D. Leykam and Y. D. Chong, *Phys. Rev. Lett.* **117**, 143901 (2016).
- [54] X. Zhou, Y. Wang, D. Leykam, and Y. D. Chong, *New J. Phys.* **19**, 095002 (2017).
- [55] L. J. Maczewsky, M. Heinrich, M. Kremer, S. K. Ivanov, M. Ehrhardt, F. Martinez, Y. V. Kartashov, V. V. Konotop, L. Torner, D. Bauer, and A. Szameit, *Science* **370**, 701 (2020).
- [56] D. Smirnova, D. Leykam, Y. Chong, and Y. Kivshar, *Appl. Phys. Rev.* **7**, 021306 (2020).
- [57] T. Tuloup, R. W. Bomantara, C. H. Lee, and J. Gong, *Phys. Rev. B* **102**, 115411 (2020).
- [58] M. Guo, S. Xia, N. Wang, D. Song, Z. Chen, and J. Yang, *Opt. Lett.* **45**, 6466 (2020).
- [59] S. Kruk, A. Poddubny, D. Smirnova, L. Wang, A. Slobozhanyuk, A. Shorokhov, I. Kravchenko, B. Luther-Davies, and Y. Kivshar, *Nat. Nanotechnol.* **14**, 126 (2019).
- [60] M. Ezawa, *Phys. Rev. B* **104**, 235420 (2021).
- [61] M. S. Kirsch, Y. Zhang, M. Kremer, L. J. Maczewsky, S. K. Ivanov, Y. V. Kartashov, L. Torner, D. Bauer, A. Szameit, and M. Heinrich, *Nat. Phys.* **17**, 995 (2021).
- [62] Y. Hadad, J. C. Soric, A. B. Khanikaev, and A. Alù, *Nature Electronics* **1**, 178 (2018).
- [63] M. Ezawa, *J. Phys. Soc. Jpn.* **91**, 024703 (2022).
- [64] F. Zangeneh-Nejad and R. Fleury, *Phys. Rev. Lett.* **123**, 053902 (2019).
- [65] R. Hirota, *J. Phys. Soc. Jpn.* **43**, 2079 (1977).
- [66] S. J. Orfanidis, *Phys. Rev. D* **18**, 3822 (1978).
- [67] M. Ezawa, *Phys. Rev. B* **100**, 165419 (2019).